Lateral and Vertical Ordering in Self-Organized PbSe Quantum Dot Superlattices

G. Springholz[1], M. Pinczolits[1], R. Lechner[1], A. Raab[1], P. Mayer[1], V. Holy[1], G. Bauer[1], H. H. Kang[2], L. Salamanca-Riba[2]

[1] Institut für Halbleiter- u. Festkörperphysik, Johannes Kepler Universität, Altenbergerstraße 69, 4040 Linz, Austria

[2] Department of Materials and Nuclear Engineering, University of Maryland, College Park, USA

Self-organized lateral and vertical ordering in PbSe/$Pb_{1-x}Eu_xTe$ quantum dot superlattices is investigated by transmission electron and atomic force microscopy. We observe the occurrence of three different ordered dot structures as a function of the $Pb_{1-x}Eu_xTe$ spacer thickness d_s, namely, (a) a vertical dot alignment with weak hexagonal ordering tendency for small d_s, (b) a well defined trigonal dot lattice with *fcc*-stacking and nearly perfect lateral ordering for intermediate d_s, and (c) uncorrelated and laterally disordered superlattices for large d_s. The formation of these different dot correlations is explained by finite element calculations.

1. Introduction

The spontaneous formation of three dimensional (3D) islands in the Stranski-Krastanow growth mode of highly lattice-mismatched heteroepitaxial layers has recently evolved as a novel technique for the fabrication of self-assembled semiconductor quantum dots [1]. Under appropriate conditions, these islands exhibit sizes in the nanometer regime and are fully coherent (*i.e.*, dislocation free) to the substrate. When embedded in a higher band gap matrix material, quantum boxes with atomic-like optical and electronic properties are formed. Due to the statistical nature of growth, these dots are usually not very uniform in size, shape and spacing, which poses severe limitations for device applications. Multilayering is one possible route for improving the uniformity of self-assembled dots [2] – [4]. This is due to the elastic interactions between the dots across the spacer layers, which leads to the formation of long-range correlations in superlattices.

In the present work, we have investigated the self-organized vertical and lateral ordering in PbSe/$Pb_{1-x}Eu_xTe$ quantum dot superlattices. It is shown that different types of correlations are formed by changes in the spacer thickness. Whereas for small spacer thicknesses, the dots are vertically aligned, an *ABCABC...* stacking sequence is formed for intermediate spacer thicknesses, and no correlations are found for thick spacer layers. The occurrence of the different structures is explained on the basis of finite element calculations of the elastic strain fields induced by the buried PbSe dots, showing a characteristic change when the spacer thickness becomes comparable to the buried dot size.

2. Experimental

A series of superlattice samples was grown by molecular beam epitaxy on PbTe buffer layers predeposited on (111) oriented BaF_2 substrates [4]. The superlattice stacks consisted of 30 periods of 5 monolayers (ML) PbSe alternating with $Pb_{1-x}Eu_xTe$ spacer layers of 200 to 1000 Å in thickness. Due to the -5.4% lattice mismatch with respect to PbTe, PbSe grows in the Stranski-Krastanow mode with the formation of 3D islands once the critical coverage of 1.5 ML is exceeded [5]. During the overgrowth of these islands, a rapid replanarisation takes place such that after 200 Å a smooth 2D surface is regained [4]. Identical growth conditions were employed for all samples with a substrate temperature of 360 ° C and growth rates of 0.08 ML/sec and 3.5 Å/sec for PbSe and $Pb_{1-x}Eu_xTe$, respectively. Thus, the only difference in the superlattices (SLs) was the thickness and composition of the spacer layers, where the latter was adjusted to provide a complete strain symmetrization of the SL stack with respect to the PbTe buffer layer [5]. This prevents misfit dislocation formation and ensures identical strain conditions in all samples.

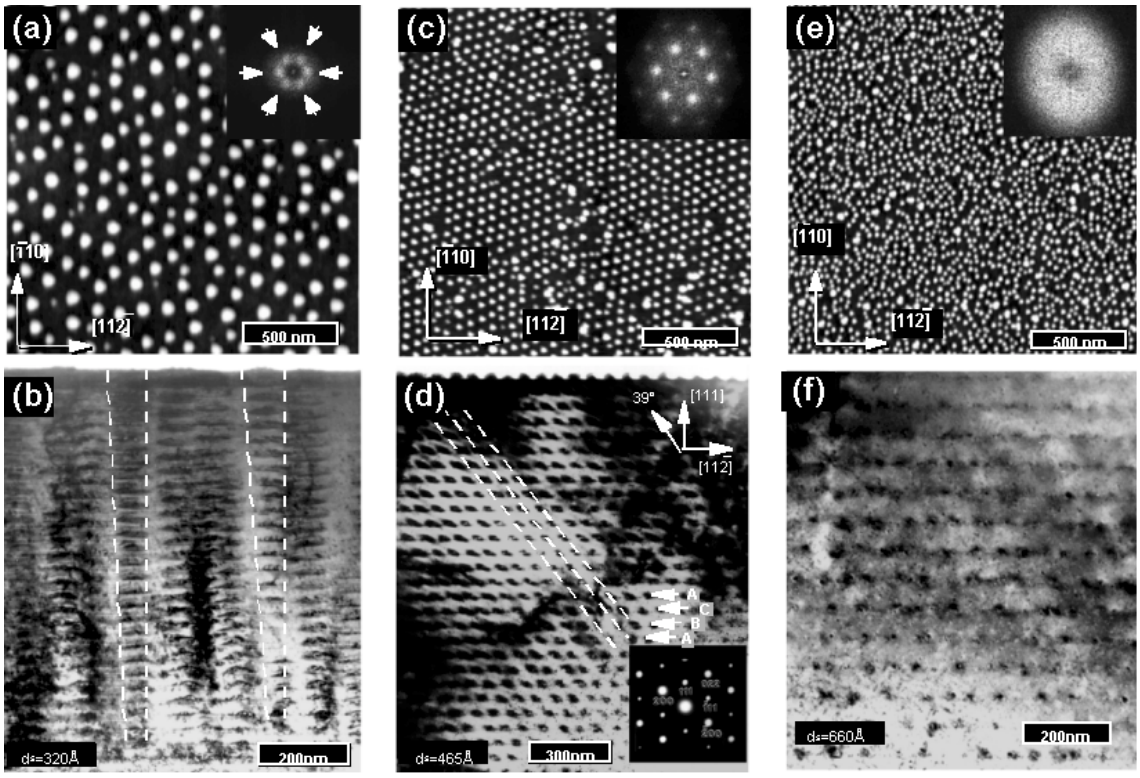

Fig. 1: AFM surface images (top) and cross-sectional TEM micrographs (bottom) of self-assembled PbSe/$Pb_{1-x}Eu_xTe$ dot superlattices with 30 superlattice periods and different $Pb_{1-x}Eu_xTe$ spacer thicknesses of d_s = 320 Å (left), 465 Å (center), and 660 Å (right hand side). For small spacer thicknesses (I) the dots are vertically aligned with weak lateral ordering tendency. For intermediate spacer thicknesses (II) a dot alignment inclined by 39° with respect to the growth direction occurs with an *fcc*-like *ABCABC*... stacking sequence and nearly perfect hexagonal lateral ordering. For thick spacers (III) no vertical dot correlations and no lateral ordering is observed. Inserts in the top panels: 2D FFT power spectra of the AFM images.

3. Results

The atomic force microscopy (AFM) images of the last dot layer and the cross sectional transmission electron microscopy (TEM) images are shown in Fig. 1 for $Pb_{1-x}Eu_xTe$ spacer thicknesses of d_s = 320, 465 and 660 Å. For small spacer thicknesses d_s < 370 Å (Fig. 1(a), (b)), as the number of superlattice periods increases larger and larger PbSe dots are formed on the surface, with a dot density decreasing from the initial value of 550 μm^{-2} for the single layers to about 70 μm^{-2} after 30 SL periods. Correspondingly, the average dot height of 180 Å and base width of 700 Å is much larger as compared to that of single dot layers grown under identical growth conditions. The cross sectional TEM image of this sample (Fig. 1(b)) reveals that the dots are vertically aligned in *columns*, is similar as in InAs/GaAs or SiGe/Si dot superlattices.

Increasing the spacer thickness to 370 – 540 Å leads to a completely different dot arrangement. As shown in Fig. 1(c), a *nearly perfect* hexagonal 2D lattice of dots is formed in this case, with a substantial narrowing of the size dispersion [4]. In addition, the dot density of about 250 μm^{-2} is about four times larger as compared to the samples with thinner spacer layers, with a corresponding decrease of the dot sizes. As demonstrated by the cross sectional TEM of Fig. 1(d), the PbSe dots are now aligned in directions *inclined* by 39° with respect to the growth direction (see dashed lines), and a well ordered trigonal 3D *lattice* of dots with a vertical *ABCABC...* stacking sequence is formed. For spacer thicknesses larger than 550 Å (Fig. 1(e) – (f)), another striking change occurs where the 2D hexagonal dot lattice is replaced by a highly disordered dot arrangement with an even higher dot density of 550 μm^{-2}. The cross-sectional TEM image of this sample (Fig. 1(f)) shows that the PbSe dots in each layer are randomly positioned relative to those in the adjacent layers. Thus, the whole SL structure just represents an uncorrelated repetition of disordered 2D single dot layers.

The different lateral ordering tendency is clearly reflected by the Fourier transformation (FFT) power spectra of the AFM images shown as insets in Fig. 1. For the sample with intermediate spacer thicknesses, many well defined satellite peaks appear in the FFT image (Fig. 1(c)). The clear six-fold symmetry and the large number of higher order peaks indicates the formation of large perfectly ordered 2D hexagonal dot domains. The exceedingly high efficiency of the lateral ordering process is corroborated by the corresponding cross-sectional TEM image, revealing that the lateral ordering sets in already within the first superlattice layers. For spacer thicknesses larger than 550 Å (Fig. 1(e)), only a diffuse ring is observed in the FFT image. This indicates the lack of any lateral ordering tendency and a rather broad dispersion of dot spacings. For samples with small spacer thicknesses $d_s \leq 370$ Å (Fig. 1(a)), although the dots seem to nucleate at random positions, six broad satellite side peaks are still visible in the FFT image (indicated by arrows in Fig. 1(a)). This indicates a weak hexagonal ordering tendency with rather large preferred lateral dot spacing. However, the absence of any higher order FFT satellites shows that only a short-range order exists in this case.

A strikingly different behavior is also found for the scaling of the preferred in-plane dot separation as a function of spacer thickness [6]. For small SL periods $D \leq 380$ Å, the lateral dot separation L is around 1300 Å, varying only slowly as $L = (0.6\ D + L_0)$ with $L_0 = 1080$ Å. At a critical period of $D_1^c = 390$ Å, L drops abruptly by a factor of three to 550 Å, and a nearly perfect 2D dot lattice is formed. In this regime, L scales *exactly* linearly with D as $L = \sqrt{3} \times D \tan \alpha$ [3], where α is the layer-to-layer correlation angle of 39° observed by TEM. For SL periods exceeding a critical value of $D_2^c = 570$ Å, the

mean lateral dot distance again drops abruptly to a value of 450 Å, and remains constant for all larger D. The corresponding dot density then equal to that of single dot layers grown under identical growth conditions. Both structural transitions are not completely abrupt, *i.e.*, for D around 390 Å actually mixed structures with coexisting trigonal and columnar dot regions are observed by TEM. Similarly, the second transition is manifested by a rapid but continuos drop of the layer-to-layer correlation probability.

The formation of different vertical correlations is explained as follows. Due to the lattice distortions around the buried dots a non-uniform strain distribution is imposed on the epitaxial surface. This leads to a preferred island nucleation at the minima of the strain energy on the surface. As shown by our previous work [3], [7], due to the very high elastic anisotropy of the IV-VI compounds and the chosen (111) growth orientation, the strain energy distribution caused by each buried PbSe dots exhibits three pronounced side minima that are laterally displaced from the surface normal direction. The preferred dot nucleation at these strain minima leads to an *ABCABC...* vertical dot stacking sequence [3] as well as to a very efficient hexagonal lateral ordering tendency. This is observed for the superlattices with intermediate spacer thicknesses. To explain the other types of dot correlations, the finite thickness of the spacer layer as well as the finite size of the buried dots has to be taken into account. For this purpose we have performed a series of finite element calculations of the stress distribution around dots located at various depths D below the surface. According to our AFM studies [5], the PbSe dots were modeled as triangular pyramids with (100) side facets. This yields an aspect ratio of b/h = 2.45, where b is the dot base width and h the dot height. Introducing the dimensionless surface coordinates $x' = x/D$ along [-110] and $y' = y/D$ along [-1-12], it turns out that the shape of the energy distribution is only determined by the ratio of D/b, *i.e.*, on the ratio of the depth to the island base width. The results of these calculations are shown in Fig. 2.

For spacer thicknesses larger than the island base $D/b > 1$, the strain energy distributions $E(x',y')$ closely resemble that obtained from a point source model [3], with three well separated minima along the <-1-12> directions. This is exemplified in Fig. 2(b) for D/b = 1.5. The directions of these minima are inclined by $\alpha = 35°$ with respect to the surface normal, in close agreement to the correlation angle observed by TEM. However, when D/b decreases below 1, α rapidly decreases to zero (as is shown in Fig. 2(c)). This means that the three minima are replaced by one central minimum located exactly above the buried dot. This is illustrated by the calculated strain energy distribution shown in Fig. 2(a) for the case of D/b = 0.5. As a consequence, preferential nucleation of new dots then occurs directly above each buried dot, which corresponds to a cross-over from *fcc* stacking to a vertical alignment of the dots, as is observed in the experiments. A more detailed analysis shows that this crossover takes place when the lateral minima separation L becomes smaller than the dot base width. Then, the island size becomes incompatible with the trigonal dot arrangement. Application of this condition to the actual parameters of our experiments leads to an expected critical spacer thickness of D_1^c = 310 Å for this transition, in good agreement with the experiments [6]. On the other hand, as the spacer thickness increases, the depth of these strain minima ΔE_{min} rapidly decreases as $1/D^3$ [6]. As a result, the layer-to-layer dot correlation probability drops to zero at a certain spacer thickness, which is experimentally the case for D_2^c = 560 Å, the upper boundary for the trigonal dot structure.

Due to the changes in the PbSe dot size as a function of the growth conditions, the positions of the critical superlattice periods D^c also change upon changes in the growth con-

ditions. In particular, at lower substrate temperatures, which result in smaller dot sizes, the phase boundaries are shifted to smaller values, which means that an *fcc*-stacking can be also obtained for SL periods smaller than 380 Å. This effect can be utilized in order to extend the tunability range of the trigonal superlattice structure.

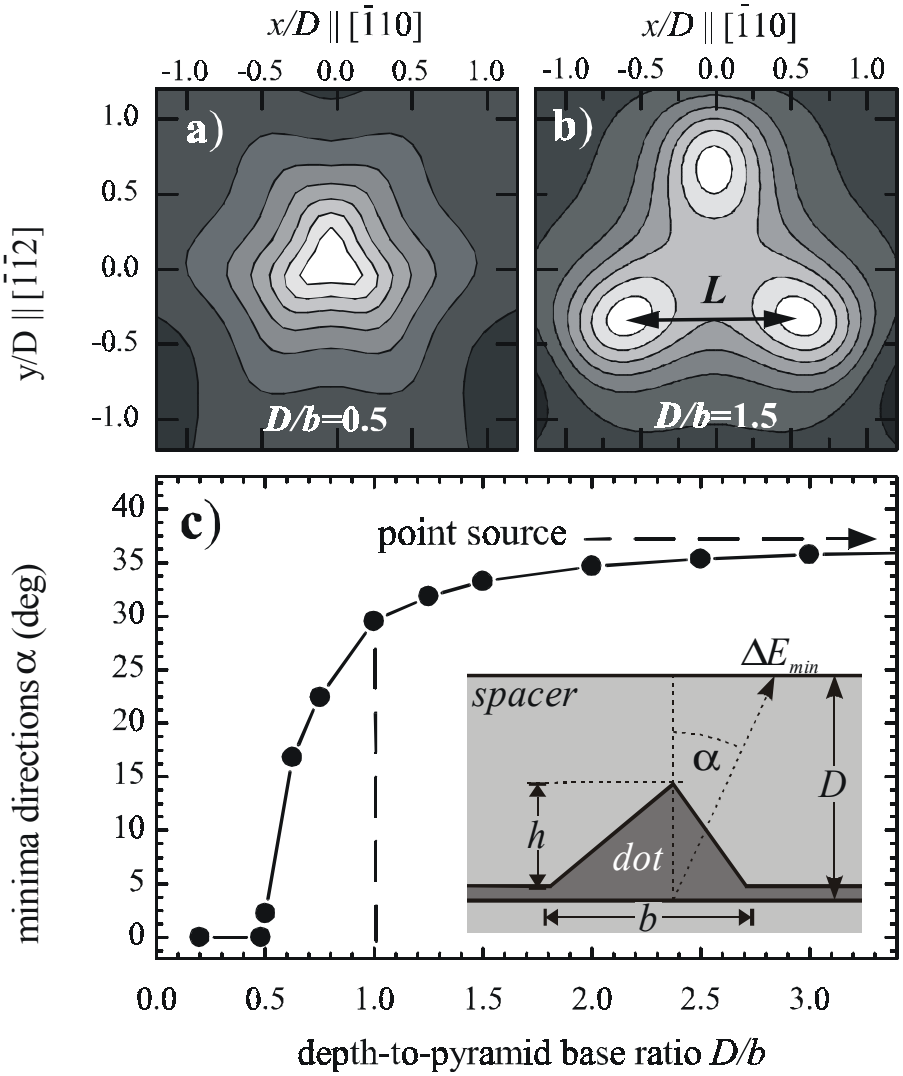

Fig. 2: Surface strain energy distributions above a pyramidal PbSe quantum dot in a PbEuTe matrix derived from finite element calculations and plotted as a function of dimensionless surface coordinates *x/D* for two different dot depths of (a) $D = 0.5 \times b$ and (b) $D = 1.5 \times b$, where *b* is the dot base width. Brighter areas in the contour plots correspond to lower strain energies. (c) Directions α of the strain energy minima on the surface relative to the surface normal plotted as a function of the *D/b* ratio. The dot configuration for the calculations is shown in (c) as insert.

4. Conclusions

In conclusion, different types of vertical correlations are observed in PbSe quantum dot superlattices as a function of the $Pb_{1-x}Eu_xTe$ spacer thickness. The different vertical cor-

relations have dramatic effects on the lateral ordering tendency as well as on the scaling of the lateral dot spacing as a function of spacer thickness. In addition, a different evolution of dot sizes and shapes occurs. The transition between the differently correlated structures is caused by the dependence of the elastic interaction between the dots on the thickness of the spacer layer, as well as by the finite lateral dot sizes. Similar trends are be expected also for other material systems.

Acknowledgements

This work is supported by the *Fonds zur Förderung der wissenschaftlichen Forschung* and the Austrian Academy of Sciences.

References

[1] D. Leonard, M. Krishnamurty, C. M. Reaves, S. P. Denbaar, and P. Petroff, Appl. Phys. Lett. 63 (1993) 3203.

[2] J. Tersoff, C. Teichert, and M.G. Lagally, Phys. Rev. Lett. 76 (1996) 1675.

[3] G. Springholz, V. Holy, M. Pinczolits, and G. Bauer, Science 282 (1998) 734.

[4] M. Pinczolits, G. Springholz, and G. Bauer, Phys. Rev. B 60 (1999) 11524.

[5] M. Pinczolits, G. Springholz, and G. Bauer, Appl. Phys. Lett. 73 (1998) 250.

[6] G. Springholz, M. Pinczolits, P. Mayer, V. Holy, G. Bauer, H. Kang, and L. Slamanca-Riba, Phys. Rev. Lett. 84 (2000) 4669.

[7] V. Holy, G. Springholz, M. Pinczolits, G. Bauer, Phys. Rev. Lett. 83 (1999) 356.